

Diffraction dijets at HERA and EIC using GTMDs

Barbara Linek^{1,2}

In collaboration with Marta Łuszczak, Wolfgang Schäfer, and Antoni Szczurek

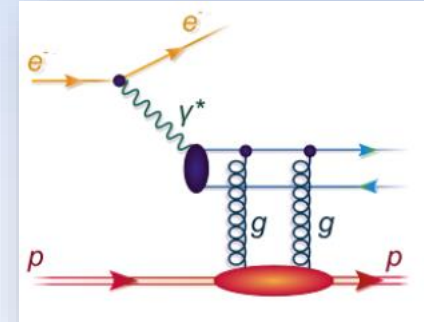
42nd International Conference of High Energy Physics

17-24 July 2024

¹Doctoral School of the University of Rzeszow, Poland ²Institute of Physics, University of Rzeszow, Poland

Introduction

- The diffractive production of high-momentum particles provides information about, among other, the unintegrated gluon distribution of the target.
- Examples of the above are Generalized transverse momentum distributions (GTMDs) derived from full transformation to the momentum space, the so-called Wigner distributions.
- In the region of small Bjorken- x GTMDs are equivalent to dipole amplitude depending on the dipole size and impact parameter.
- GTMDs depend on the transverse momentum transfer and the transverse momentum of a parton in the proton or nucleus, including a dependence on the azimuthal angle between the two transverse vectors. It is therefore possible to distinguish the so-called elliptic GTMD.
- It is possible to study the elliptic gluon distributions in diffractive reactions such as exclusive dijet production in ep collisions, pA and AA ultra-peripheral collisions (UPC), or exclusive $Q\bar{Q}$ photo-production in pA and AA UPC.
- In this analysis, six different models of GTMD are referenced to the experimental data.

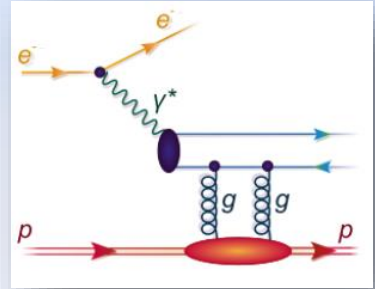
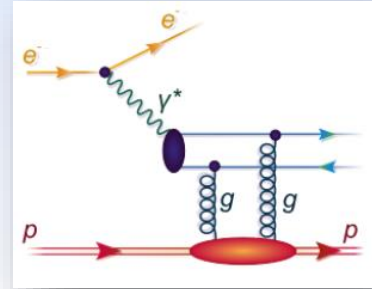
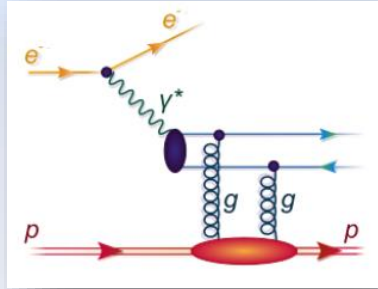
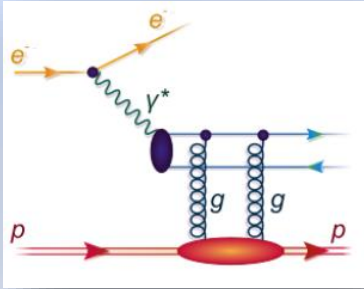


$$\vec{P}_{\perp} = \frac{1}{2} (\vec{p}_{\perp Q} - \vec{p}_{\perp \bar{Q}})$$

$$\vec{\Delta}_{\perp} = \vec{p}_{\perp Q} + \vec{p}_{\perp \bar{Q}}$$

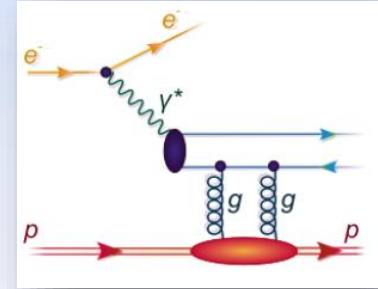
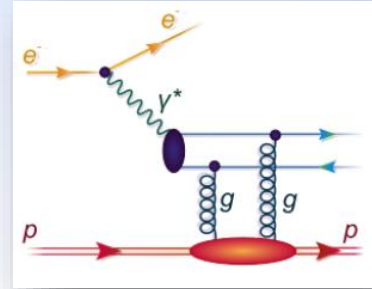
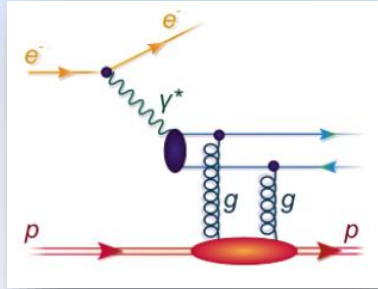
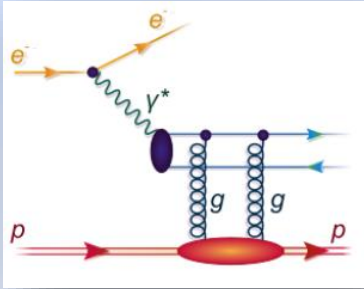
$$\cos\phi = \frac{\vec{P}_{\perp} \cdot \vec{\Delta}_{\perp}}{P_{\perp} \Delta_{\perp}}$$

Diffractive photo-production of $q\bar{q}$ in electron-proton collisions



$$\frac{d\sigma^{ep}}{dydQ^2dzd^2\vec{P}_\perp d^2\vec{\Delta}_\perp} = \frac{\alpha_{em}}{\pi y Q^2} \left[\left(1 - y + \frac{y^2}{2}\right) \frac{d\sigma_T^{\gamma^*p}}{dzd^2\vec{P}_\perp d^2\vec{\Delta}_\perp} + (1 - y) \frac{d\sigma_L^{\gamma^*p}}{dzd^2\vec{P}_\perp d^2\vec{\Delta}_\perp} \right]$$

Diffractive photo-production of $q\bar{q}$ in electron-proton collisions



$$\frac{d\sigma_T^{\gamma^*p}}{dzd^2\vec{P}_\perp d^2\vec{\Delta}_\perp} = 2N_c\alpha_{em} \sum_f e_f^2 \int d^2\vec{k}_\perp \int d^2\vec{k}'_\perp T(Y, \vec{k}_\perp, \vec{\Delta}_\perp) T(Y, \vec{k}'_\perp, \vec{\Delta}_\perp)$$

$$\times \left\{ (z^2 + (1-z)^2) \left[\frac{(\vec{P}_\perp - \vec{k}_\perp)}{(P_\perp - \vec{k}_\perp)^2 + \epsilon^2} - \frac{\vec{P}_\perp}{P_\perp^2 - \epsilon^2} \right] \cdot \left[\frac{(\vec{P}_\perp - \vec{k}'_\perp)}{(P_\perp - \vec{k}'_\perp)^2 + \epsilon^2} - \frac{\vec{P}_\perp}{P_\perp^2 - \epsilon^2} \right] + m_f^2 \left[\frac{1}{(P_\perp - \vec{k}_\perp)^2 + \epsilon^2} - \frac{1}{P_\perp^2 - \epsilon^2} \right] \cdot \left[\frac{1}{(P_\perp - \vec{k}'_\perp)^2 + \epsilon^2} - \frac{1}{P_\perp^2 - \epsilon^2} \right] \right\}$$

$$\frac{d\sigma_L^{\gamma^*p}}{dzd^2\vec{P}_\perp d^2\vec{\Delta}_\perp} = 2N_c\alpha_{em} 4Q^2 z^2 (z-1)^2 \times \sum_f e_f^2 \int d^2\vec{k}_\perp \int d^2\vec{k}'_\perp T(Y, \vec{k}_\perp, \vec{\Delta}_\perp) T(Y, \vec{k}'_\perp, \vec{\Delta}_\perp)$$

$$\times \left[\frac{1}{(P_\perp - \vec{k}_\perp)^2 + \epsilon^2} - \frac{1}{P_\perp^2 - \epsilon^2} \right] \cdot \left[\frac{1}{(P_\perp - \vec{k}'_\perp)^2 + \epsilon^2} - \frac{1}{P_\perp^2 - \epsilon^2} \right]$$

$$\epsilon^2 = z(1-z)Q^2 + m_f^2$$

Fourier transform of dipole amplitude

The gluon density matrix encodes the same information as the Fourier transform of the dipole amplitude, up to the term containing δ – function

$$f\left(Y, \frac{\vec{\Delta}_\perp}{2} + \vec{k}_\perp, \frac{\vec{\Delta}_\perp}{2} - \vec{k}_\perp\right) \rightarrow \frac{1}{2} T(Y, \vec{k}_\perp, \vec{\Delta}_\perp), \quad T(Y, \vec{k}_\perp, \vec{\Delta}_\perp) = \int \frac{d^2\vec{b}_\perp}{(2\pi)^2} \frac{d^2\vec{r}_\perp}{(2\pi)^2} e^{-i\vec{\Delta}_\perp \cdot \vec{b}_\perp} e^{-i\vec{k}_\perp \cdot \vec{r}_\perp} N(Y, \vec{r}_\perp, \vec{b}_\perp)$$

which is clearly visible in the form

$$T(Y, \vec{k}_\perp, \vec{\Delta}_\perp) = C(Y, \vec{\Delta}_\perp) \left(\delta^2\left(\vec{k}_\perp - \frac{\vec{\Delta}_\perp}{2}\right) + \delta^2\left(\vec{k}_\perp + \frac{\vec{\Delta}_\perp}{2}\right) \right) - f\left(Y, \frac{\vec{\Delta}_\perp}{2} + \vec{k}_\perp, \frac{\vec{\Delta}_\perp}{2} - \vec{k}_\perp\right) - f\left(Y, \frac{\vec{\Delta}_\perp}{2} - \vec{k}_\perp, \frac{\vec{\Delta}_\perp}{2} + \vec{k}_\perp\right)$$

This transform is non-convergent, therefore it needs to be regularized by inserting a Gaussian cutoff function:

$$T(Y, \vec{k}_\perp, \vec{\Delta}_\perp) = \int \frac{d^2\vec{b}_\perp}{(2\pi)^2} \frac{d^2\vec{r}_\perp}{(2\pi)^2} e^{-i\vec{\Delta}_\perp \cdot \vec{b}_\perp} e^{-i\vec{k}_\perp \cdot \vec{r}_\perp} N(Y, \vec{r}_\perp, \vec{b}_\perp) e^{-\epsilon r_\perp^2}$$

or, using δ – function with $\delta_\epsilon^2(\vec{k}_\perp) = \frac{1}{4\pi\epsilon} \exp\left(-\frac{\vec{k}_\perp^2}{4\epsilon}\right)$

$$T(Y, \vec{k}_\perp, \vec{\Delta}_\perp) = C(Y, \vec{\Delta}_\perp) \left(\delta_\epsilon^2\left(\vec{k}_\perp - \frac{\vec{\Delta}_\perp}{2}\right) + \delta_\epsilon^2\left(\vec{k}_\perp + \frac{\vec{\Delta}_\perp}{2}\right) \right) - f_\epsilon\left(Y, \frac{\vec{\Delta}_\perp}{2} + \vec{k}_\perp, \frac{\vec{\Delta}_\perp}{2} - \vec{k}_\perp\right) - f_\epsilon\left(Y, \frac{\vec{\Delta}_\perp}{2} - \vec{k}_\perp, \frac{\vec{\Delta}_\perp}{2} + \vec{k}_\perp\right)$$

Fourier transform of dipole amplitude

The leading dependence on dipole orientation may be quantified by the elliptic part of the dipole amplitude in the Fourier expansion:

$$N(Y, \vec{r}_\perp, \vec{b}_\perp) = N_0(Y, r_\perp, b_\perp) + 2\cos(2\phi_{br})N_\epsilon(Y, r_\perp, b_\perp) + \dots$$

Therefore, the isotropic and elliptic parts of the dipole amplitude to GTMDs are translated by the appropriate Fourier-Bessel transforms:

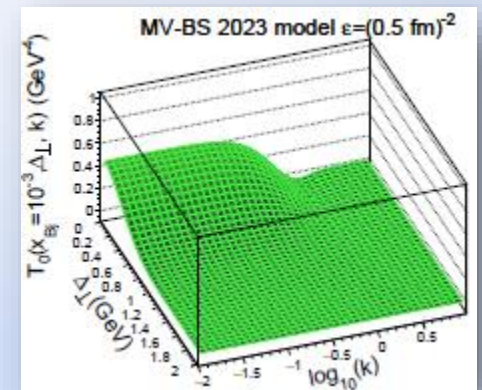
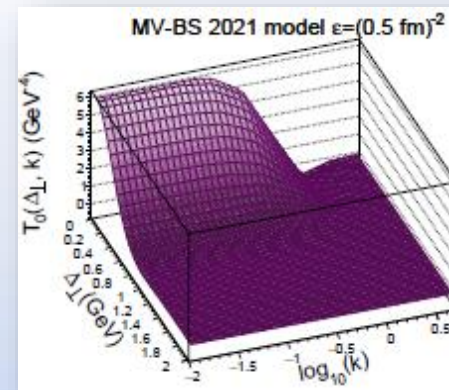
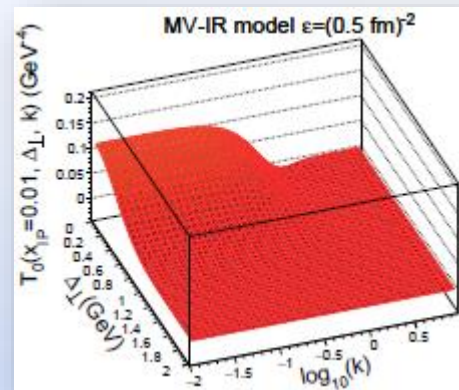
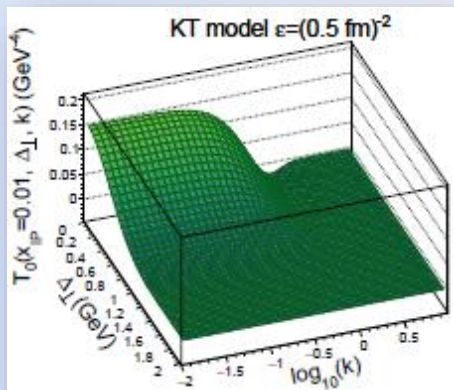
$$T_0(Y, k_\perp, \Delta_\perp) = \frac{1}{4\pi^2} \int_0^\infty b_\perp db_\perp J_0(\Delta_\perp b_\perp) \int_0^\infty r_\perp dr_\perp J_0(k_\perp r_\perp) N_0(Y, r_\perp, b_\perp) e^{-\epsilon_r r_\perp^2}$$
$$T_\epsilon(Y, k_\perp, \Delta_\perp) = \frac{1}{4\pi^2} \int_0^\infty b_\perp db_\perp J_2(\Delta_\perp b_\perp) \int_0^\infty r_\perp dr_\perp J_2(k_\perp r_\perp) N_\epsilon(Y, r_\perp, b_\perp) e^{-\epsilon_r r_\perp^2}$$

KT, MV-IR, MV-BS parametrizations

Parametrizations based on the regularized Fourier transform of dipole amplitude are as follows:

- **The Kowalski – Teaney (KT) model**, which has been adjusted to the proton structure function data but does not include dipole orientation effects;
- **The MV – IR model**, which is based on the original effective McLerran-Venugopalan model independent of the Y , therefore we used a formula including additional dependence: $T_{MV-IR}^{mod}(Y, \vec{k}_\perp, \vec{\Delta}_\perp) = T_{MV-IR}(Y, \vec{k}_\perp, \vec{\Delta}_\perp) e^{\lambda Y}$, $Y = \ln\left(\frac{0.01}{x_{\mathbb{P}}}\right)$, $\lambda = 0.277$;
- **The MV – BS 2021 model**, which is also independent of the Y but is adapting to the experimental data by introducing: $\chi = 1.25$ in the following equation:

$$N_0(r_\perp, b_\perp) = -\frac{1}{4} r_\perp^2 \chi Q_s^2(b_\perp) \ln\left[\frac{1}{r_\perp^2 \lambda^2} + e\right]$$
 with $Q_s^2(b_\perp) = \frac{4\pi\alpha_s C_F}{N_C} \exp\left[-\frac{b_\perp^2}{2R_p^2}\right]$;
- **The MV – BS 2023 model**, which is a newer version of the MV-BS 2021 and depends on the x_{Bj} by replacing the χ factor with: $\chi(x_{Bj}) = \bar{\chi} \left(\frac{0.0001}{x_{Bj}}\right)^{\lambda_\chi}$, where $\bar{\chi} = 1.5, \lambda_\chi = 0.29$;

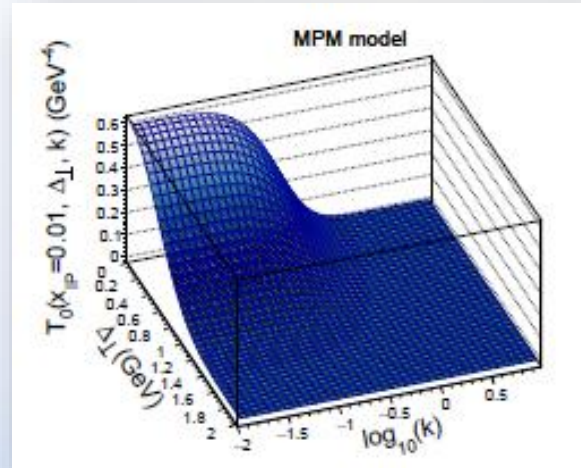
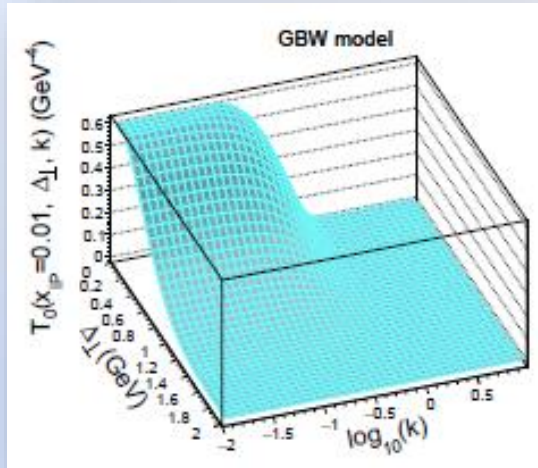


MPM and GBW parametrizations

Two different parametrizations of the off-forward gluon density matrix were used in the calculation:

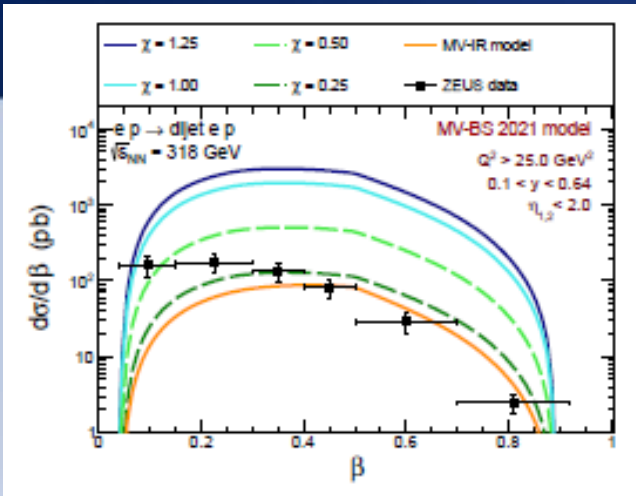
$$f\left(Y, \frac{\vec{\Delta}_\perp}{2} + \vec{k}_\perp, \frac{\vec{\Delta}_\perp}{2} - \vec{k}_\perp\right) = \frac{\alpha_s}{4\pi N_C} \frac{\mathcal{F}(x_{\mathbb{P}}, \vec{k}_\perp, -\vec{k}_\perp)}{\vec{k}_\perp^4} \exp\left[-\frac{1}{2} B \vec{\Delta}_\perp^2\right]$$

In both – the Golec-Biernat–Wüsthoff (GBW) model and the Moriggi–Peccini–Machado (MPM) model, the diffractive slope equals $B = 4 \text{ GeV}^{-2}$.



$$f\left(Y, \frac{\vec{q}_\perp}{2} + \vec{k}_\perp, \frac{\vec{q}_\perp}{2} - \vec{k}_\perp\right) \rightarrow \frac{1}{2} T(Y, \vec{k}_\perp, \vec{\Delta}_\perp)$$

H1 and ZEUS kinematics

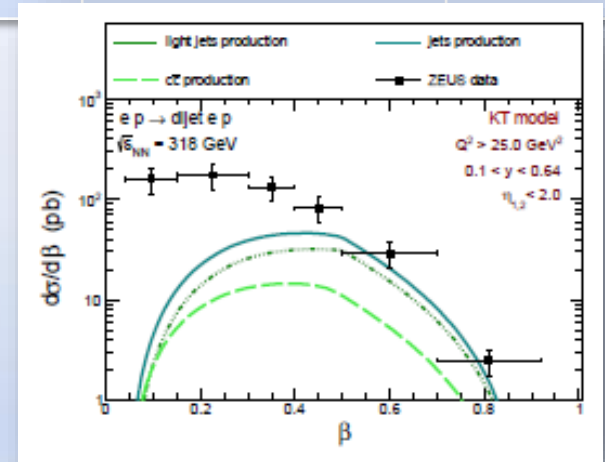
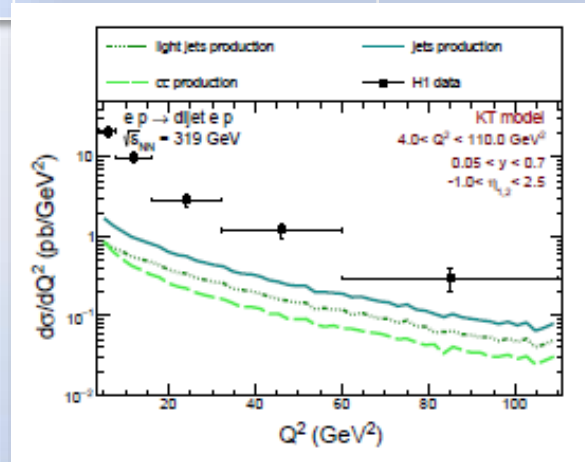


HERA cuts

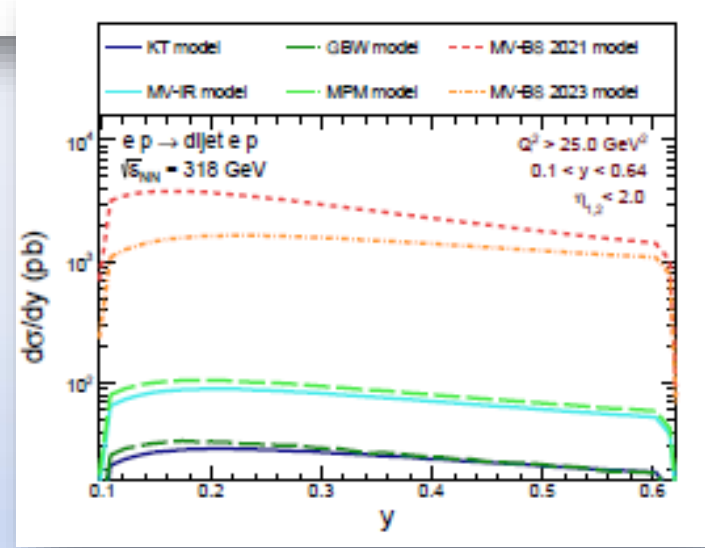
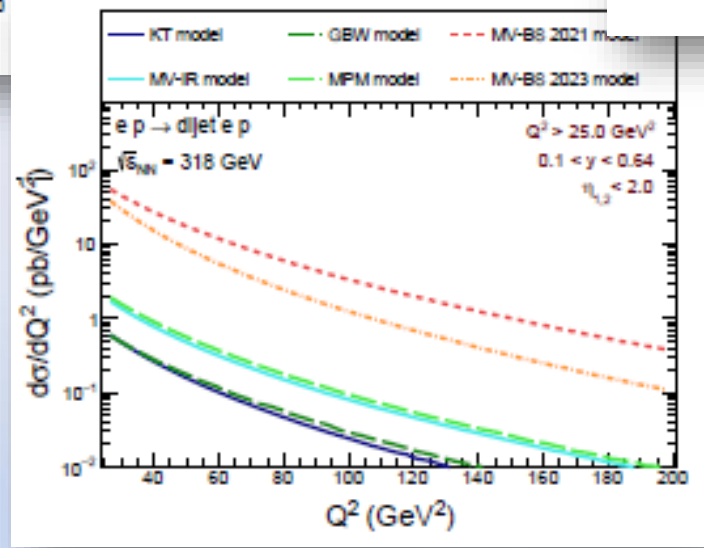
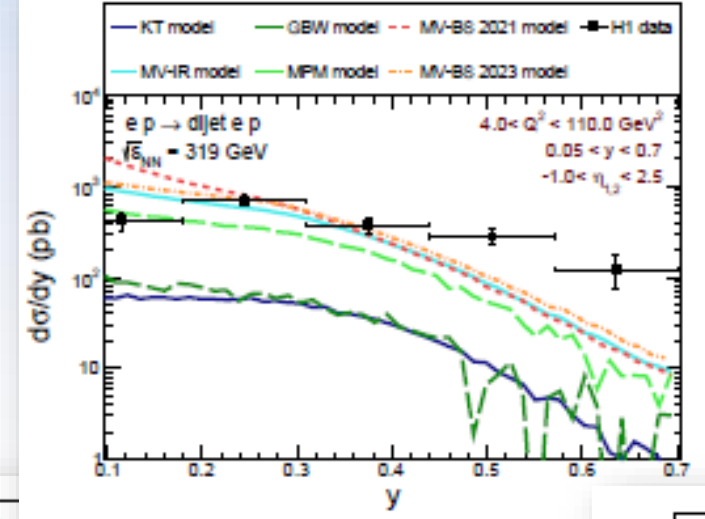
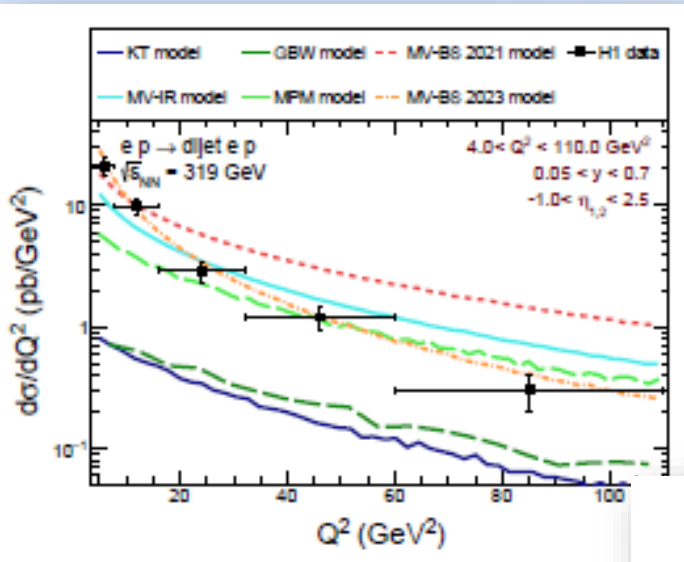
| H1 | ZEUS |
|-------------------------------|---------------------------------------|
| $4 < Q^2 < 110 \text{ GeV}^2$ | $Q^2 > 25 \text{ GeV}^2$ |
| $x_{IP} < 0.1$ | $x_{IP} < 0.01$ |
| $0.05 < y < 0.7$ | $0.1 < y < 0.64$ |
| $-1 < \eta_{1,2} < 2.5$ | $\eta_{1,2} < 2$ |
| $p_{\perp 1} > 5 \text{ GeV}$ | $p_{\perp 1,2} > 2 \text{ GeV}$ |
| $p_{\perp 2} > 4 \text{ GeV}$ | $M_{jj} > 5 \text{ GeV}$ |
| $ t < 1 \text{ GeV}^2$ | $90 < W_{\gamma p} < 250 \text{ GeV}$ |

| GTMD approaches | H1 cuts, $\sigma(\text{pb})$ | | |
|-----------------|------------------------------|---------------------------|-------------------------|
| | light $q\bar{q}$ | $ep \rightarrow c\bar{c}$ | no $p_{\perp 1,2}$ cuts |
| GBW | 26.35 | 19.91 | 10900.86 |
| MPM | 147.94 | 108.26 | 10151.00 |
| KT | 21.29 | 15.20 | 5957.65 |
| MV – IR | 243.20 | 155.21 | 11784.75 |
| MV – BS 2021 | 404.06 | 269.75 | 10999.73 |
| MV – BS 2023 | 288.34 | 189.74 | 6685.82 |
| DATA | 254 | | |

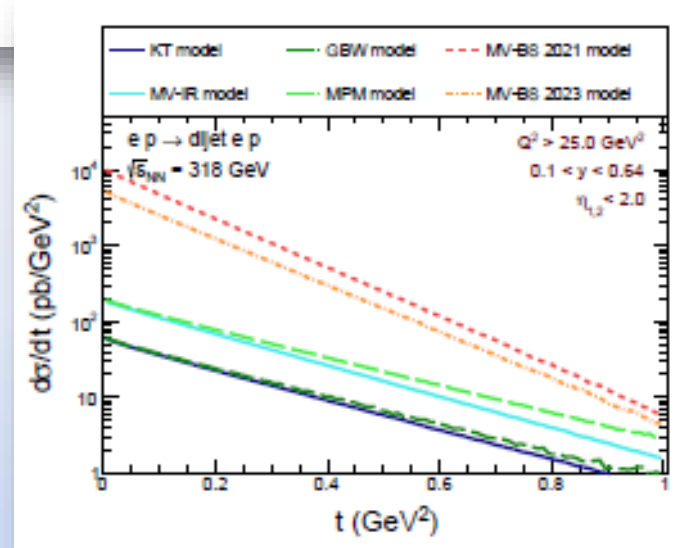
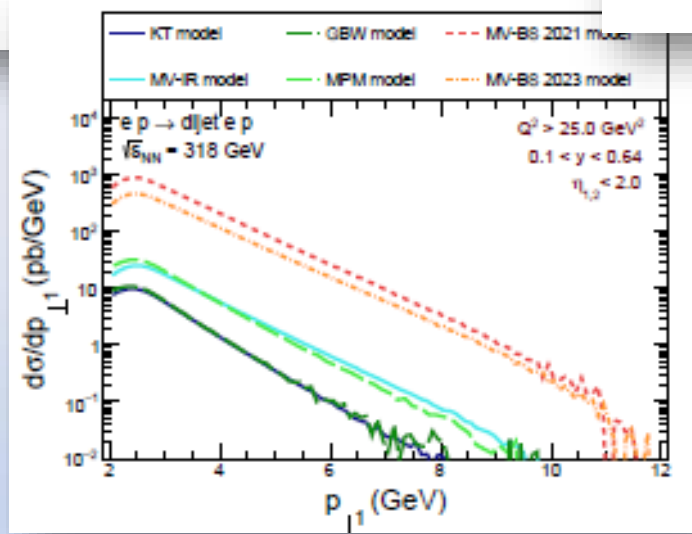
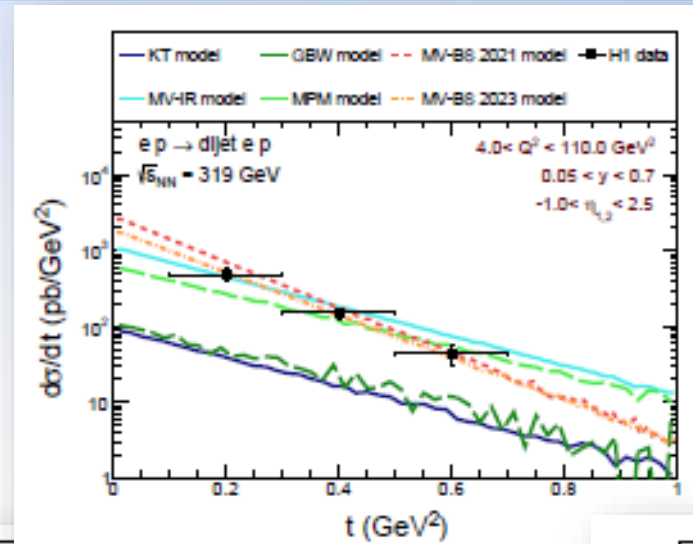
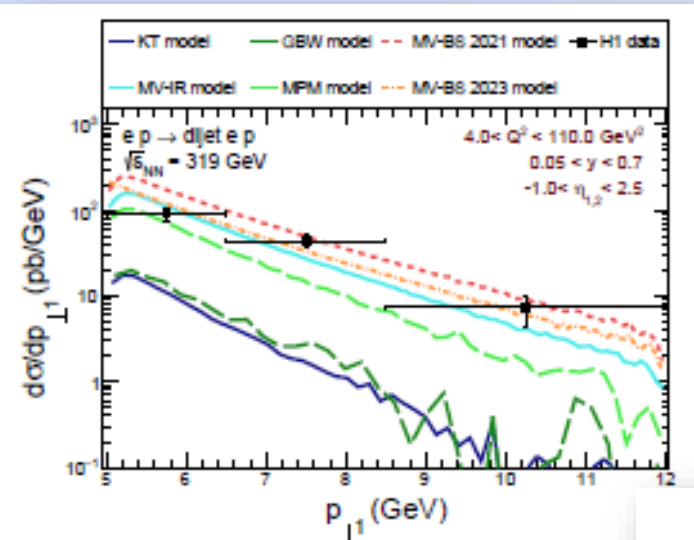
| GTMD approaches | ZEUS cuts, $\sigma(\text{pb})$ | | |
|-----------------|--------------------------------|---------------------------|-------------------------|
| | light $q\bar{q}$ | $ep \rightarrow c\bar{c}$ | no $p_{\perp 1,2}$ cuts |
| GBW | 13.57 | 6.67 | 337.11 |
| MPM | 43.61 | 20.47 | 313.17 |
| KT | 12.57 | 5.67 | 52.60 |
| MV – IR | 37.83 | 17.62 | 91.18 |
| MV – BS 2021 | 1346.11 | 624.55 | 3117.95 |
| MV – BS 2023 | 732.15 | 348.40 | 1510.33 |
| DATA | 72 | | |



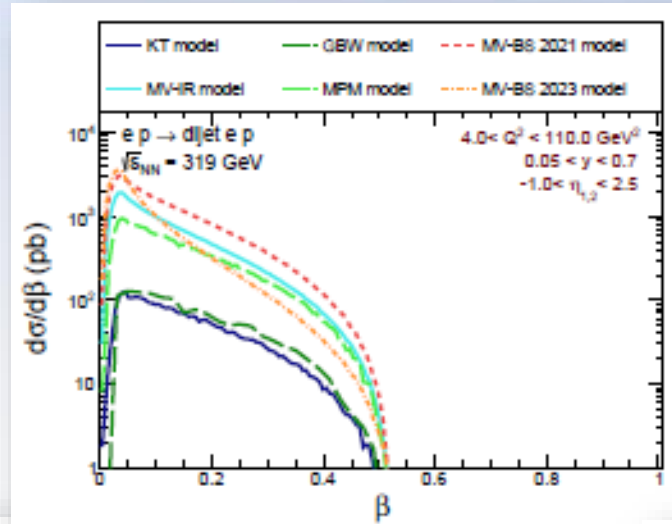
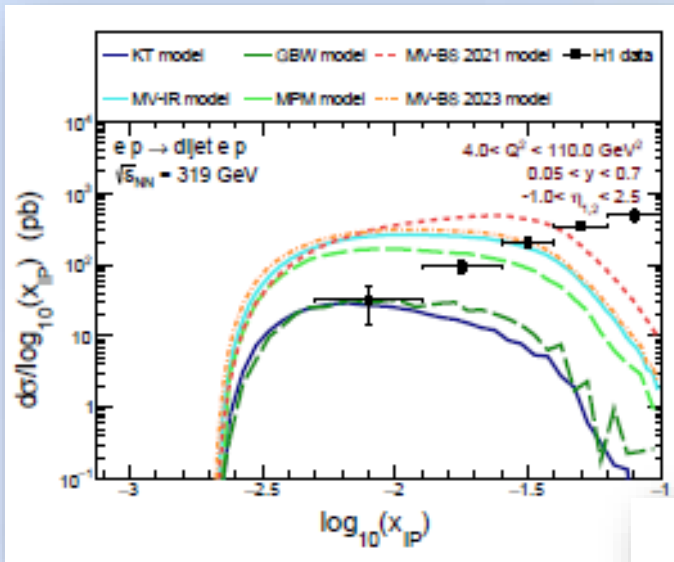
Distributions in Q^2 and y



Distributions in $p_{\perp 1}$ and t

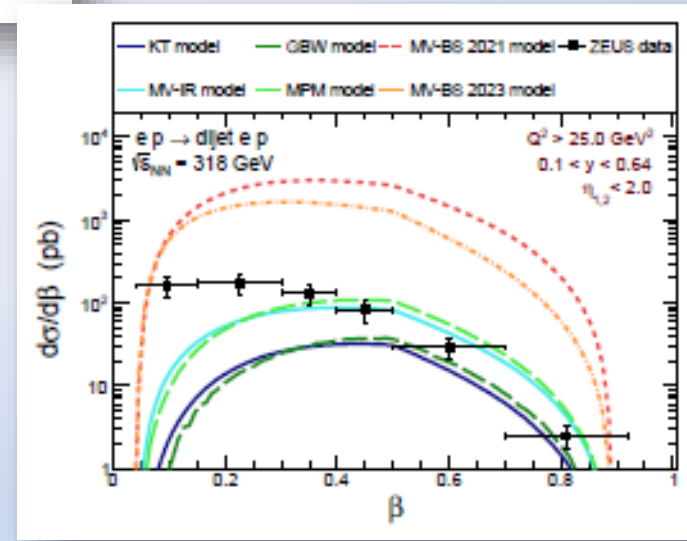
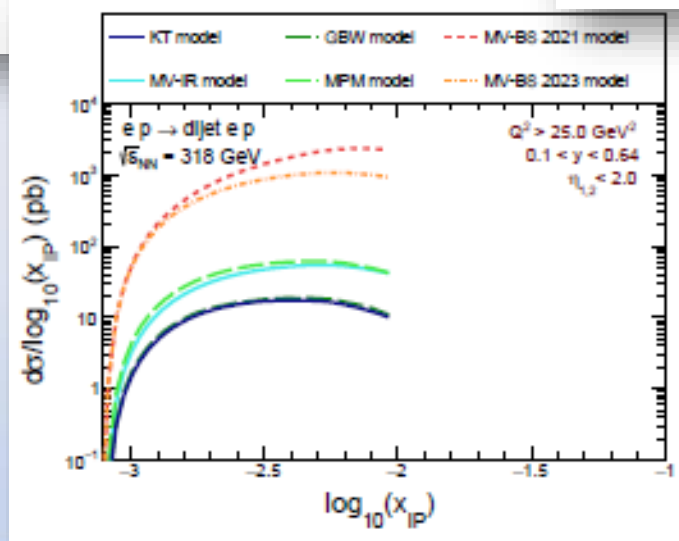


Distributions in $\log_{10}(x_{IP})$ and β

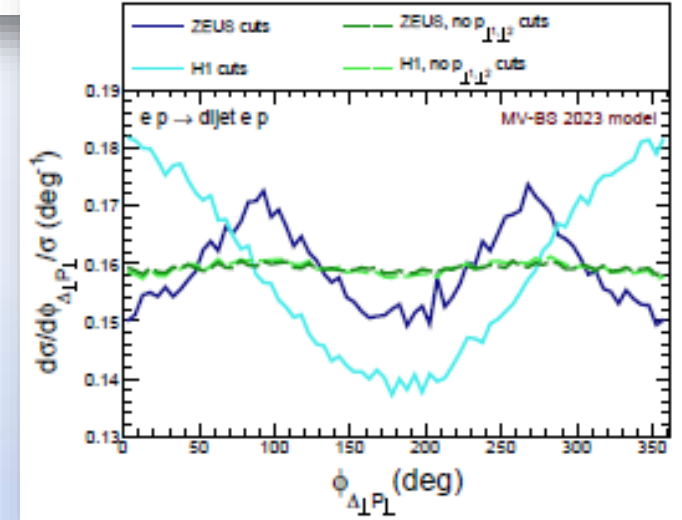
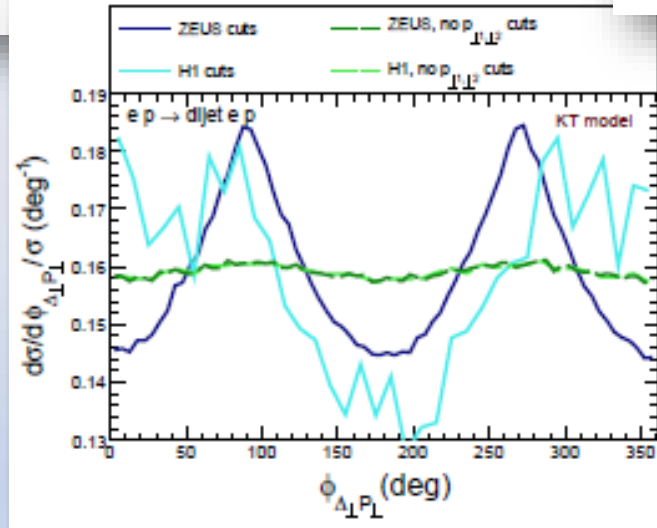
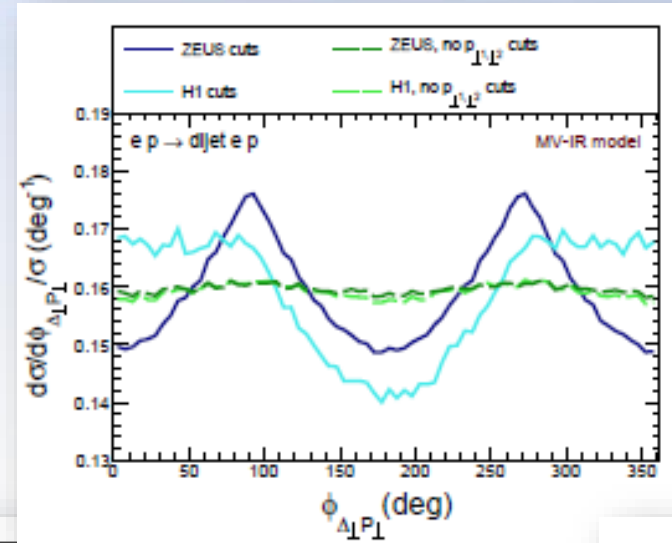
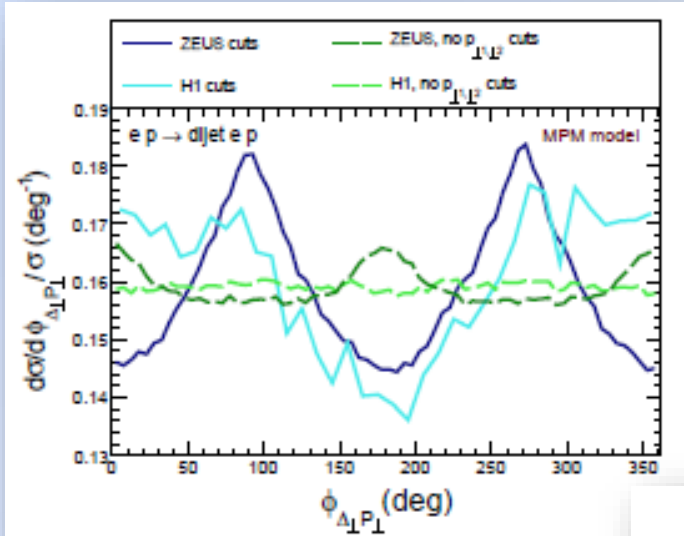


$$\beta = \frac{Q^2}{Q^2 + M_{jj}^2}$$

$$M_{jj}^2 = \frac{p_{\perp 1}^2 + m_q^2}{z} + \frac{p_{\perp 2}^2 + m_q^2}{1-z} - \Delta_{\perp}^2$$



Distributions in $\phi_{\Delta_{\perp} P_{\perp}}$



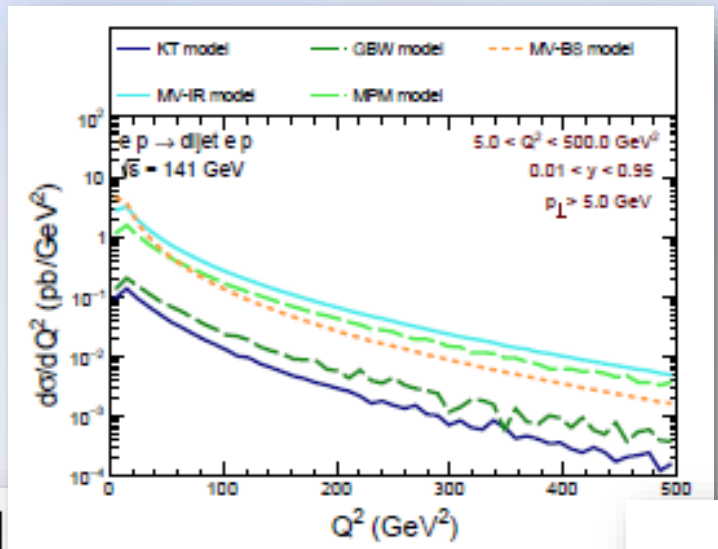
$$\vec{P}_{\perp} = \frac{1}{2}(\vec{p}_{\perp Q} - \vec{p}_{\perp \bar{Q}})$$

$$\vec{\Delta}_{\perp} = \vec{p}_{\perp Q} + \vec{p}_{\perp \bar{Q}}$$

$$\cos\phi = \frac{\vec{P}_{\perp} \cdot \vec{\Delta}_{\perp}}{P_{\perp} \Delta_{\perp}}$$

EIC predictions

| GTMD model | σ (pb) |
|------------|---------------|
| GBW | 10.93 |
| MPM | 77.89 |
| KT | 6.53 |
| MV - IR | 144.15 |
| MV - BS | 136.49 |



including cuts

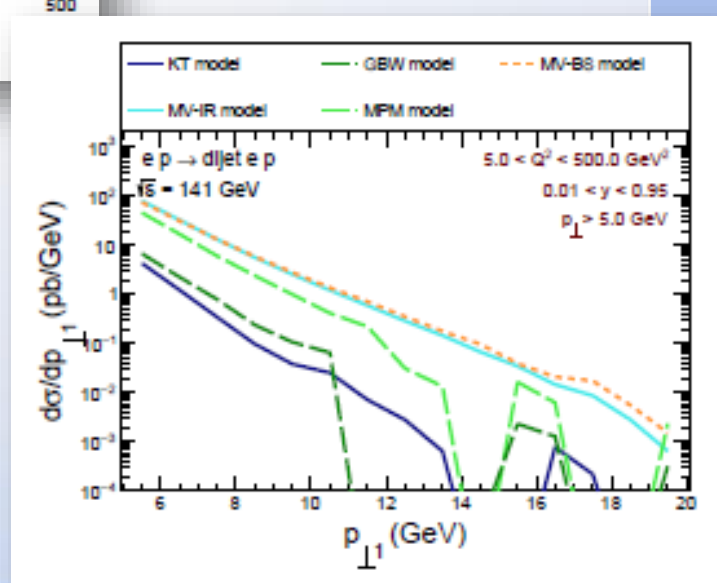
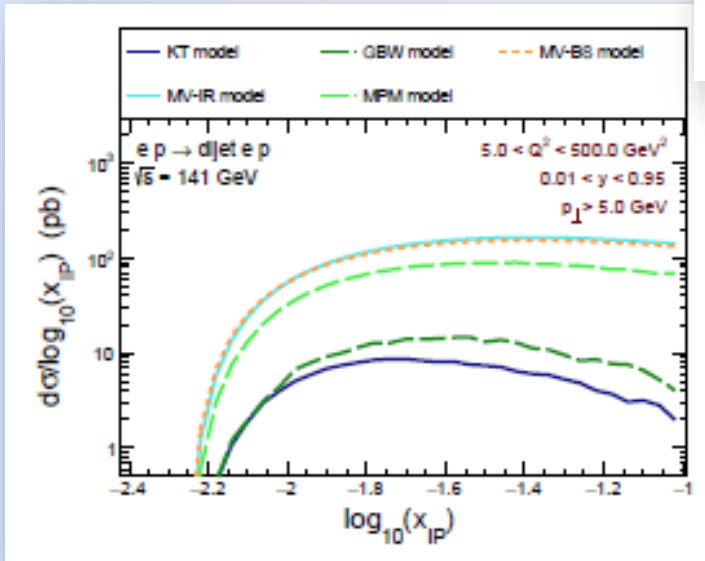
$\sqrt{s} = 141 \text{ GeV}$
 $E_e = 18.8 \text{ GeV}$,
 $E_p = 275 \text{ GeV}$

$p_{\perp 1,2} > 5 \text{ GeV}$

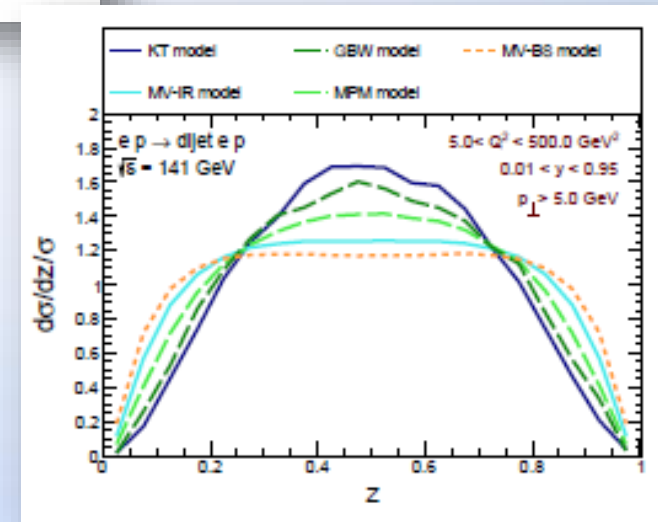
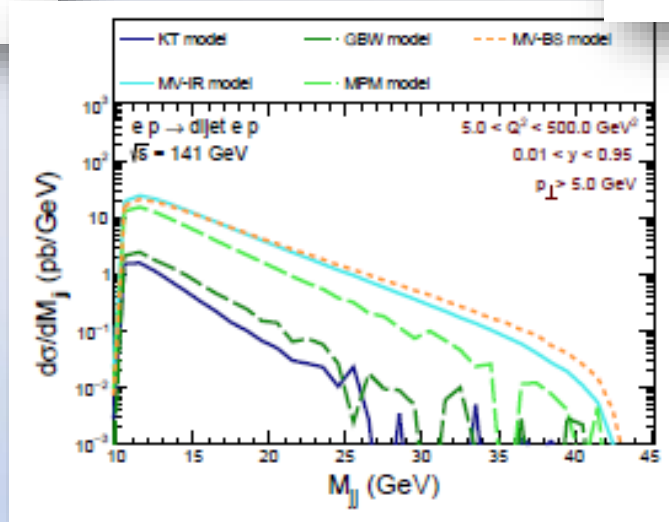
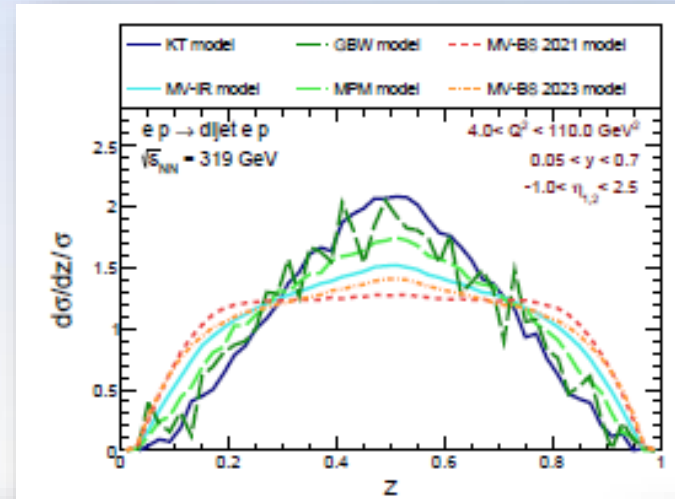
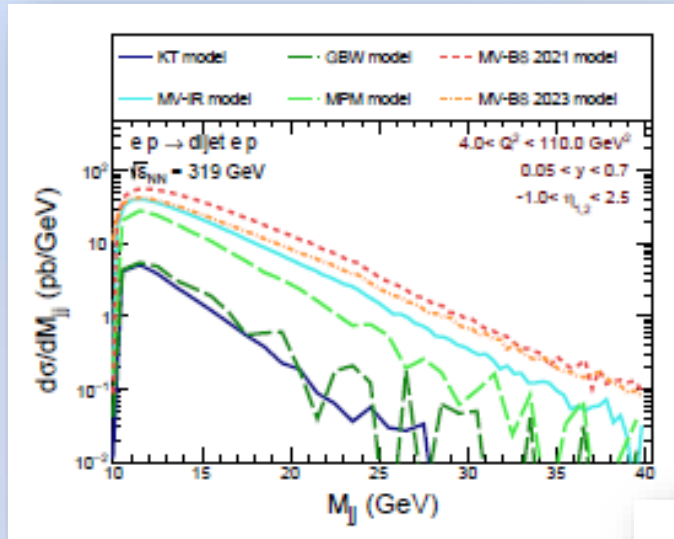
$0.01 < y < 0.95$

$-3.5 < \eta_{1,2} < 3.5$

$5.0 > Q^2 > 500 \text{ GeV}^2$



EIC predictions



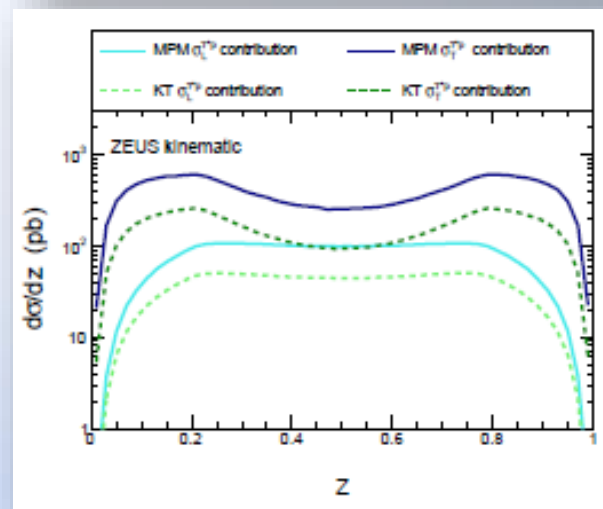
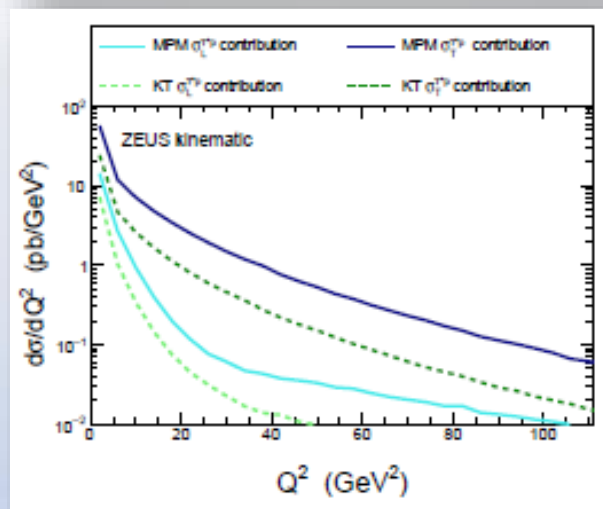
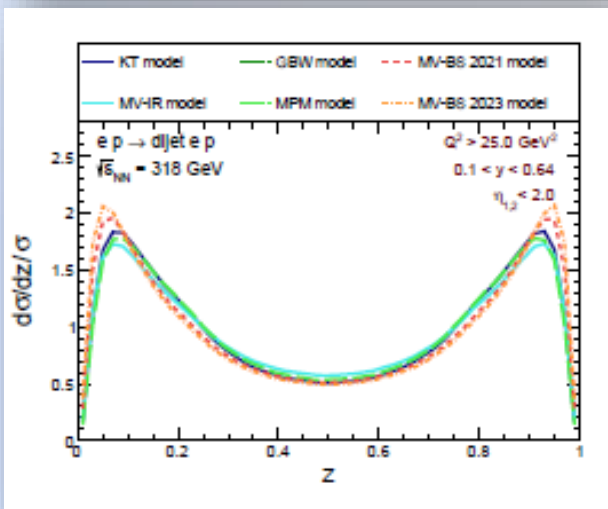
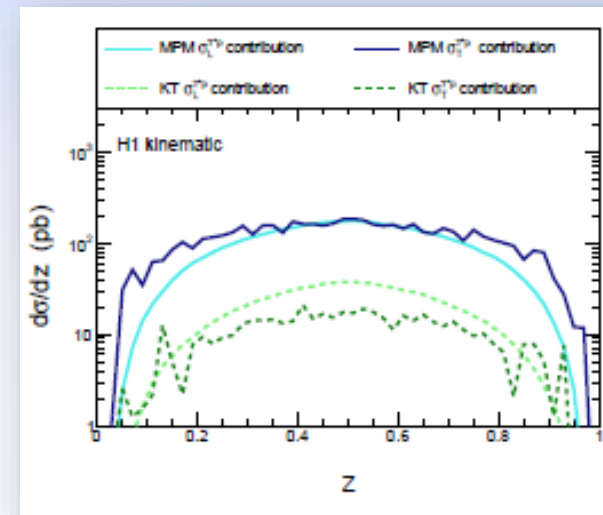
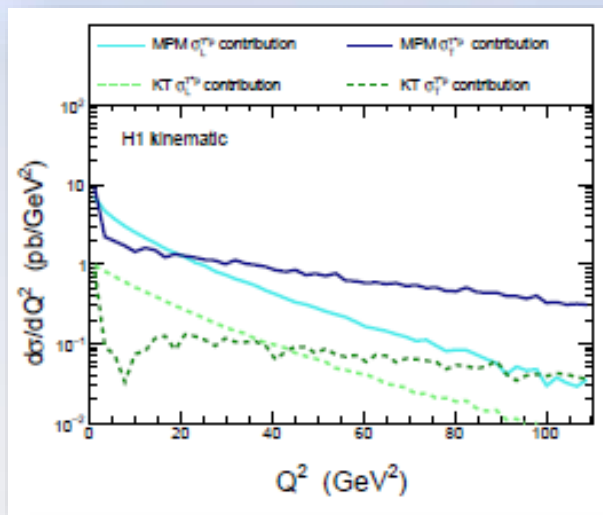
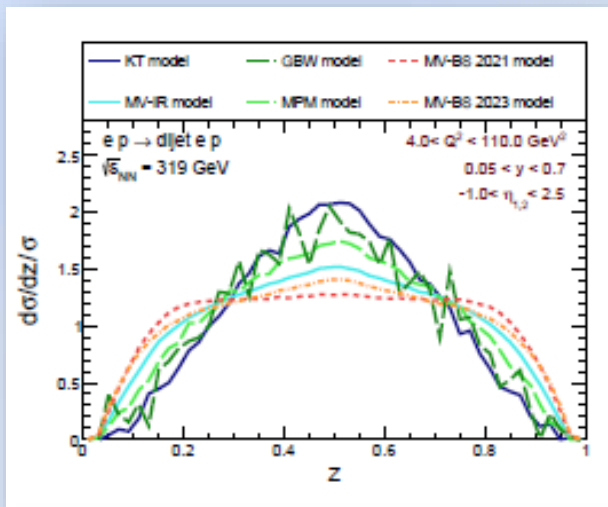
Conclusions

- Several differential distributions for the diffractive photo-production of dijets in $ep \rightarrow e jj p$ reaction at LHC energies have been presented.
- Models based on the Fourier transform of the dipole matrices were regularized by an extra factor, that leads to rather large uncertainties as far as normalization of the cross-section is concerned.
- Special attention has been paid to azimuthal correlations. However, the found correlations result only from geometric dependencies, hence they may cause erroneous interpretations.
- The MV-BS, MPM, and MV-IR GTMDs models reasonably well describe many observables for the H1 kinematics, but fail to describe distributions in x_{IP} distribution and strongly overshoot the cross-section differential in β for the ZEUS kinematics.
- Predictions for the EIC kinematics are also presented, which are quite similar to the H1 kinematics due to similar cuts. However, the much higher luminosity of the new accelerator will contribute to a much more accurate fit of the models used to the experimental data, which will, of course, also require taking into account other processes.

Thank you for your attention

Additional slides

Distributions in z



Dependence of the MV-IR model on the factor ϵ

